Geophys. J. Int. (2002) **150,** 285–294

LITH5.0: a revised crustal model for Canada based on Lithoprobe results

H. K. C. Perry,[1,*] D. W. S. Eaton[1] and A. M. Forte[1]

[1]*Department of Earth Sciences, The University of Western Ontario, London, Ontario, Canada. E-mail: perry@ipgp.jussieu.fr*

Accepted 2002 February 19. Received 2002 February 5; in original form 2001 May 8

SUMMARY

During the last 15 yr, numerous seismic refraction experiments have been conducted over the Canadian landmass, most as part of the Lithoprobe initiative. The new results provide the basis for revising existing global models of crustal structure, e.g. CRUST5.1 (Mooney *et al.* 1998), which do not incorporate the new Lithoprobe data. The crustal model discussed here, LITH5.0, combines the Lithoprobe and CRUST5.1 data to provide better constraints on crustal structure in Canada. The objectives of the study are to: (1) compile available new data into a single, consistent database of crustal thickness and velocity, including the uppermost mantle (*Pn*) velocity; and (2) to construct a revised $5^\circ \times 5^\circ$ crustal model of the Canadian landmass, in a format that is generally compatible with existing global models. The Lithoprobe results suggest a 5.5 km average root mean square (rms) crustal thickness difference between LITH5.0 and CRUST5.1. Even with the incorporation of the new data, the geographic coverage in north and central Canada remains sparse. The new model does not explicitly incorporate geological constraints, but instead relies on spherical spline interpolation for extrapolating values into regions that lack control. To illustrate the implications of this new crustal model, we use LITH5.0 to correct for the isostatically compensated crustal heterogeneity in order to obtain improved estimates of the dynamic surface topography. The latter provides important constraints on the density structure of the uppermost mantle.

Key words: crustal thickness, dynamic topography, Lithoprobe, seismic refraction, spherical spline interpolation.

1 INTRODUCTION

The stability of continental crust over geological time requires that it must exceed a critical thickness to survive, and have a buoyancy high enough such that subduction is prevented (e.g. Shapiro *et al.* 1999). Knowledge of crustal thickness is therefore essential in understanding the processes of its growth and evolution. There are a wide range of applications for a model of seismic velocity and density structure of the Earth's crust and uppermost mantle. Many seismic analyses use data sets which are sensitive to crustal structure, but are unable to resolve details within the crust. For example, seismic tomographic models are sensitive to crustal structure, and it is important to apply crustal corrections which are as accurate as possible, if determination of regional-scale upper-mantle features is desired (e.g. Grand *et al.* 1997; Ekström & Dziewonski 1998; Mégnin & Romanowicz 2000). In addition, accurate crustal thickness and velocity models are necessary for constraining earthquake hypocentres. Lateral variations in mantle density may be inferred from geodynamic data (e.g. dynamic topography, gravity anomalies) if the density structure of the crust is well known (e.g. Forte *et al.* 1993, 1995; Pari & Peltier 2000; Forte & Perry 2000; Kaban & Mooney 2001).

Previous global crustal models have provided varying degrees of resolution. Soller *et al.* (1982) produced a map of crustal thickness, however, they did not include seismic velocities or densities. Hahn *et al.* (1984) presented a model of crustal structure using irregularly shaped regions of uniform structure. Tanimoto (1995) used a wide range of seismic data to evaluate crustal structure, and Nataf & Ricard (1996) presented a model of the crust and upper mantle (3SMAC) on a $2^\circ \times 2^\circ$ scale using both seismological data and non-seismological constraints. Most recently, Mooney *et al.* (1998) presented a global crustal model, CRUST5.1, which combined existing seismic refraction data published in the period 1948–1995, and compilations of ice and sediment thickness.

With the availability of new seismic data sets from the Canadian Lithoprobe programme (Clowes *et al.* 1999), we have compiled a revised database of crustal structure for Canada, LITH5.0, which is based on both new results and those previously published in CRUST5.1. Although the LITH5.0 model does not provide higher resolution than CRUST5.1 ($5^\circ \times 5^\circ$), we find that the differences

*Now at: Laboratoire de Dynamique des Systèmes Géologiques, Institut de Physique du Globe de Paris, Paris, France.

between the models in some regions of Canada are large and therefore important if the goal is to resolve large-scale lithospheric mantle structure beneath the North American craton. The goal of this study is to integrate new Lithoprobe data with the existing framework provided by CRUST5.1 such that improved predictions of isostatic and dynamic contributions to surface geodynamic observables may be obtained.

2 DATA COMPILATION

Existing global models of crustal structure contain data for Canada that entirely predate the Lithoprobe programme. Thus this work focuses on the new Lithoprobe refraction data sets in an attempt to place further constraints on crustal structure in North America following previous summaries of crustal structure (Mooney & Braile 1989; Mooney 1989; Holbrook *et al.* 1992; Christensen & Mooney 1995). The CRUST5.1 model parametrizes the crystalline continental crust into three layers; upper, middle and lower crust, and assigns to each an average *P*- and *S*-wave velocity and density. We adopted a different approach to construct the LITH5.0 model, by defining crustal thickness (not including sediments) and surface, lower crustal and *Pn* velocity. In addition, we defined depths to specific *P*-wave velocity surfaces, namely 6.4, 6.8 and 7.2 km s^{-1}. We chose these velocity surfaces since they provide a reasonable sampling of the upper, middle and lower crust. In refraction studies where seismic anisotropy was detected in the *Pn* velocity, (e.g. Németh & Hajnal 1998), the mean value was recorded in LITH5.0. In most cases however, there were insufficient data to reliably constrain the extent of anisotropy in the subcrustal mantle. In addition, recognizing the highly non-uniform distribution of control points, with dense concentrations in some regions and sparse control elsewhere (particularly in northern regions), we used spherical spline interpolation to estimate values on a uniform grid of points. The spherical spline approach was preferred because it can be applied to data sets to produce a smooth model which is well-behaved even in regions devoid of measurements. LITH5.0 consists of an irregular distribution of control points derived directly from crustal refraction surveys and a set of spherical spline coefficients and gridded data values.

Published velocity models were used to obtain control points in areas where Lithoprobe crustal refraction surveys have been performed. We chose not to include near-vertical incidence reflection data or receiver-function data in this compilation, as they do not provide direct determinations of the *P*-wave velocity–depth structure. One of the important applications of this model is in the calculation of surface crustal loads which are required in the prediction of dynamic surface topography and free-air gravity anomalies. These surface loads were calculated by vertical integration of density over depth, and thus accurate *P*-wave velocity–depth structure was essential. Velocity models were sampled geographically every 1 deg where possible. Spherical spline interpolation was useful for determining a single, representative velocity–depth pair where numerous values of seismic velocity and depth were available within a single $5° \times 5°$ cell. Spatial averaging of the velocity models was performed to remove short-wavelength (<500 km) inhomogeneities in the model through the implementation of our interpolation scheme. This approach yielded $N = 217$ new control points, from seismic refraction data, the locations of which are plotted in Fig. 1. Note that most of these new points fall between 50° and 60° latitude, and in the northern Canadian Cordillera. It is in these regions that our interpretations will focus.

Quality factors were assigned to all depth measurements: a quality factor of one corresponds to an estimated error of 5 per cent of the measurement; a quality factor of two corresponds to an estimated error of 7 per cent of the measurement; a quality factor of three corresponds to an estimated error of 10 per cent of the measurement. The quality factors used in determining the uncertainty in the crustal thickness measurement were found to be distributed such that 80 per cent of the measurements were of quality one; 14 per cent of quality two; and 6 per cent of quality three. Refraction surveys conducted prior to 1990 were assigned velocity errors of ± 0.2 km s^{-1}, while surveys conducted post 1990 were assigned errors of ± 0.1 km s^{-1} unless indicated otherwise in the individual manuscripts containing the velocity models. The new model differs from CRUST5.1 in that it is less dependent on statistical averages of crustal structure for various geological settings, such as Precambrian shields or extended continental crust. In the LITH5.0 model, Lithoprobe refraction data replaces many of the geologically constrained $5° \times 5°$ cells of CRUST5.1 where seismic data was previously unavailable. In cells where no Lithoprobe data or (older) seismic data is available, LITH5.0 relies on the geological averages provided by CRUST5.1.

3 CRUSTAL MODEL

LITH5.0 is a crustal model that incorporates *P*-wave velocity at the surface and in the lower crust, and the *Pn* velocity, in addition to depths to constant velocity surfaces (6.4, 6.8, 7.2 km s^{-1}) where they exist. The model is structured on a $5° \times 5°$ grid, and incorporates new Lithoprobe data with the previously existent CRUST5.1 data. The LITH5.0 model is summarized in Table 1. Table 1 lists the crustal thickness and depths to constant velocity surfaces, in addition to the surface, lower crust and *Pn* velocities in all $5° \times 5°$ cells in Canada containing Lithoprobe data.

Spherical spline interpolation is well suited to interpolation with smooth basis functions onto a spherical reference surface from an irregular distribution of control points (Parker 1994). The spherical spline predictions and the measured values in regions constrained by Lithoprobe data were found to be in good agreement, with a maximum difference of about 1 per cent, where control points were assigned errors equivalent to the average rms difference between the CRUST5.1 and LITH5.0 models. The rms error, ε, was calculated relative to CRUST5.1 in cells where crustal thickness was known from the Lithoprobe results using

$$\varepsilon = \sqrt{\frac{\sum_{i=1}^{N}(\mathrm{h}_{\mathrm{LITH5.0}} - \mathrm{h}_{\mathrm{CRUST5.1}})^2}{N}} \tag{1}$$

Weighting functions required in the interpolation were applied to the data and varied depending on their source. All of the CRUST5.1 data in Canada were given a relative weight equivalent to their average rms error, ε, whereas the LITH5.0 data were given weights according to the quality of the data and the year in which the refraction survey was carried out.

Wherever possible, depths of the velocity surfaces 6.4, 6.8 and 7.2 km s^{-1}, the surface velocity, the lower crustal velocity and the *Pn* velocity were recorded from velocity–depth functions extracted from published crustal interpretations. Figs 2(a) and (b) show the depth in kilometres of the 6.4 and 6.8 km s^{-1} *P*-wave velocity surfaces, respectively. In some instances, the crust does not contain any velocity values greater than 6.4 or 6.8 km s^{-1}, in which case the velocity surface was not considered for that cell. The lower crustal velocities are illustrated in Fig. 2(c). Fig. 2(d) shows the *Pn*

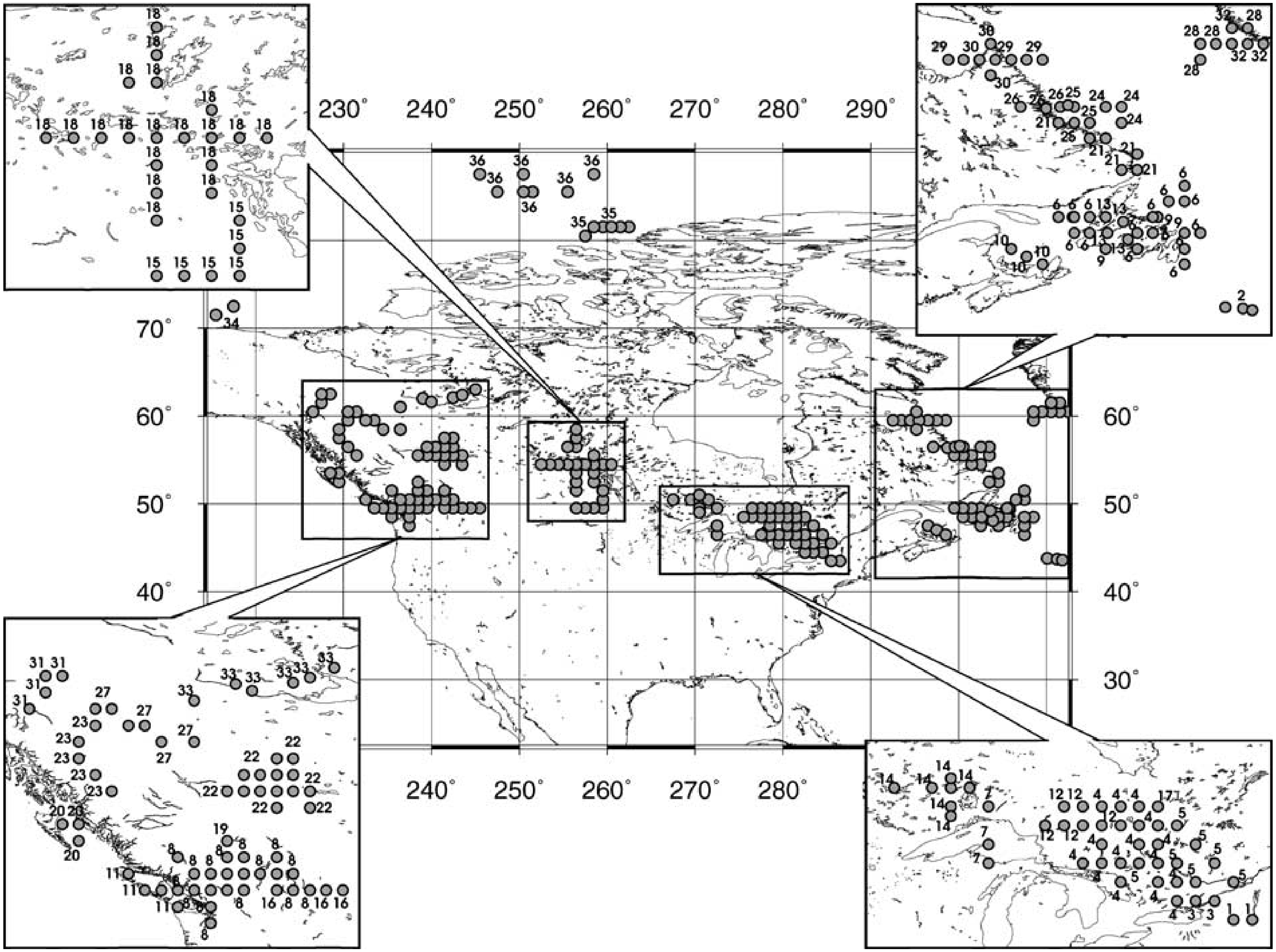

Figure 1. Locations of Lithoprobe seismic refraction lines, with the exception of the 2 northern-most surveys, which were carried out through the Geological Survey of Canada. These data provide constraints on the compressional wave seismic velocity structure, and in some cases the shear wave structure although the latter was not utilized in this study. Data selection and uncertainties are discussed in the text. The numbers correspond to the sources of published data: [1] Hughes & Luetgert (1992), [2] Reid (1994), [3] Zelt *et al*. (1994), [4] Winardhi & Mereu (1997), [5] Mereu *et al.* (1986), [6] Marillier *et al.* (1994), [7] Epili & Mereu (1989), [8] Clowes *et al.* (1995), [9] Hall *et al.* (1998), [10] Marillier & Reid (1990), [11] McMechan & Spence (1983), [12] Boland & Ellis (1991), [13] Hughes *et al.* (1994), [14] Musacchio & White (personal communication 2001), [15] Delandro & Moon (1982), [16] Zelt & White (1995), [17] Grandjean *et al.* (1995), [18] Németh & Hajnal (1998), [19] Zelt *et al.* (1992), [20] Spence & Asudeh (1993), [21] Louden & Fan (1998), [22] Zelt & Ellis (1989), [23] Hammer & Clowes (1999), [24] Chian *et al.* (1995), [25] Reid (1996), [26] Funck *et al.* (2000b), [27] Welford *et al.* (2001), [28] Chian & Louden (1994), [29] Funck & Louden (1999), [30] Funck *et al.* (2000a), [31] Creaser & Spence (2000), [32] Chian & Louden (1992), [33] Fernández Viejo & Clowes (2002), [34] Mair & Lyons (1981), [35] Asudeh *et al.* (1989), [36] Asudeh *et al.* (1988).

Table 1. The LITH5.0 crustal model for Canada. Crustal thickness in km, depths to various constant *P*-wave velocity surfaces (6.4, 6.8 and 7.2 km s^{-1}) in km, crustal *P*-wave surface velocity, the maximum lower crustal *P*-wave velocity and the *Pn* velocity in 5° × 5° cells where Lithoprobe seismic refraction data is available in Canada. The references are those from published results based on the Lithoprobe seismic refraction studies. The crustal thickness does not include sediment layers. The errors associated with the delineation of the Moho boundary are generally between 5 and 10 per cent of the total thickness. Errors associated with the delineation of *P*-wave velocity depths are generally within 0.1–0.2 km s^{-1} as given in the individual velocity models.

Location (°E, °N)	Constant velocity surface depths (km)			*P*-wave velocities (km s^{-1})			Crustal thickness (km)	Reference(s)
	6.4 (km s^{-1})	6.8 (km s^{-1})	7.2 (km s^{-1})	Surface	Lower crust	*Pn*		
282.5, 42.5	6.7	27.7		6.1	7.0	8.3	43.3	Zelt *et al*. (1994) Winardhi & Mereu (1997)
287.5, 42.5	1.7	22.5		5.4	7.1	8.1	37.3	Hughes & Luetgert (1992)
312.5, 42.5	12.7			5.9	6.7	7.9	5.2	Reid (1994)
232.5, 47.5	7.5	21.0		6.0	6.8	7.8	6.8	McMechan & Spence (1982) Clowes *et al.* (1995)
237.5, 47.5	8.1	15.4		6.0	7.0	7.7	41.0	McMechan & Spence (1982) Clowes *et al.* (1995)
242.5, 47.5	21.7			5.9	6.6	7.9	36.9	Clowes *et al.* (1995) Zelt & White (1995)
247.5, 47.5	20.1			6.3	6.5	8.0	42.1	Zelt & White (1995)
257.5, 47.5	11.6			5.9	6.5	7.9	43.4	Delandro & Moon (1982)
272.5, 47.5	10.0	37.7		5.7	6.9	8.1	56.3	Epili & Mereu (1989)
277.5, 47.5	11.9	25.8		6.2	7.1	8.1	41.8	Boland & Ellis (1991) Winardhi & Mereu (1997)
282.5, 47.5	10.0	31.4		6.0	7.0	8.1	37.9	Mereu *et al.* (1986) Grandjean *et al.* (1995) Winardhi & Mereu (1997)
287.5, 47.5	1.4	30.6	39.3	5.8	7.2	8.0	38.7	Mereu *et al.* (1986)
297.5, 47.5	13.5	15.1		5.9	6.9	8.1	38.4	Marillier & Reid (1990) Marillier *et al.* (1994) Hall *et al.* (1998)
302.5, 47.5	19.8	27.2		6.0	6.9	8.1	37.4	Hughes *et al.* (1994) Marillier *et al.* (1994) Hall *et al.* (1998)
307.5, 47.5	10.8			6.0	6.7	8.2	35.0	Hughes *et al.* (1994) Marillier *et al.* (1994) Hall *et al.* (1998)
227.5, 52.5	4.4	13.3		5.8	7.0	8.1	6.8	Spence & Asudeh (1993)
232.5, 52.5	3.3	17.0		5.7	6.8	7.6	34.1	McMechan & Spence (1982)
237.5, 52.5	15.1			6.1	6.7	7.9	32.9	Zelt *et al.* (1992) Clowes *et al.* (1995)
242.5, 52.5	19.9			5.9	6.7	8.1	36.4	Zelt & Ellis (1989)
252.5, 52.5	16.6	37.3		6.3	7.0	8.2	45.8	Németh & Hajnal (1998)
257.5, 52.5	15.7			6.2	6.7	8.2	41.5	Delandro & Moon (1982) Németh & Hajnal (1998)
262.5, 52.5	9.9	40.0	41.0	6.3	7.4	8.2	41.9	Németh & Hajnal (1998)
302.5, 52.5	9.9			5.9	6.7	8.0	46.2	Louden & Fan (1998)
307.5, 52.5	8.9	16.9		6.3	6.8	8.3	28.6	Marillier *et al.* (1994) Hall *et al.* (1998)
227.5, 57.5	17.4			6.1	6.7	7.9	32.3	Hammer & Clowes (1999)
232.5, 57.5	16.0			5.9	6.7	8.0	35.7	Hammer & Clowes (1999) Welford *et al.* (2001)
237.5, 57.5	17.4	29.6		6.0	7.1	7.9	35.8	Zelt & Ellis (1989) Welford *et al.* (2001)
242.5, 57.5	12.5	28.2	35.7	6.0	7.3	8.2	41.4	Zelt & Ellis (1989)
257.5, 57.5	17.0	18.0		6.2	7.0	8.2	40.4	Németh & Hajnal (1998)
292.5, 57.5	15.0	26.6		5.8	7.0	8.1	48.2	Funck & Louden (1999) Funck *et al.* (2000b)

Table 1. (*Continued.*)

Location (°E, °N)	Constant velocity surface depths (km)			*P*-wave velocities (km s^{-1})			Crustal thickness (km)	Reference(s)
	6.4 (km s^{-1})	6.8 (km s^{-1})	7.2 (km s^{-1})	Surface	Lower crust	*Pn*		
297.5, 57.5	11.5			5.9	6.7	8.1	36.8	Chian *et al.* (1995) Louden & Fan (1998) Funck & Louden (1999) Funck *et al.* (2000b) Funck *et al.* (2000a)
302.5, 57.5	5.7			6.1	6.7	8.0	6.8	Chian *et al.* (1995) Reid (1996) Funck *et al.* (2000a)
307.5, 57.5	1.7	3.0	4.5	5.9	7.2	8.0	5.8	Chian & Louden (1994)
227.5, 62.5	27.1	34.3		5.8	6.9	8.0	35.1	Creaser & Spence (2000)
232.5, 62.5	19.8	28.0		5.8	6.8	7.8	34.2	Welford *et al.* (2001)
237.5, 62.5	22.5	29.3		5.8	6.9	8.2	31.1	Fernández Viejo & Clowes (2002)
242.5, 62.5	17.8	25.0		5.9	7.0	8.3	33.5	Fernández Viejo & Clowes (2002)
247.5, 62.5	17.3	25.0		5.9	6.9	8.3	34.8	Fernández Viejo & Clowes (2002)
297.5, 62.5	9.7	21.7		5.9	7.0	8.1	20.4	Funck *et al.* (2000b)
307.5, 62.5	1.5	2.0	3.2	5.6	7.3	8.0	23.2	Chian & Louden (1994)
312.5, 62.5	9.5	18.6		5.8	7.0	8.0	36.1	Chian & Louden (1992) Chian & Louden (1994)
217.5, 72.5	1.1	5.0		6.6	6.8	7.6	5.1	Mair & Lyons (1981)
257.5, 82.5				5.8	6.3	8.0	15.3	Asudeh *et al.* (1989)
262.5, 82.5				5.8	6.3	8.0	17.5	Asudeh *et al.* (1989)
247.5, 87.5	1.0	5.0	15.5	6.3	7.3	8.2	17.9	Asudeh *et al.* (1988)
252.5, 87.5	1.1	4.0	17.0	6.3	7.3	8.3	21.7	Asudeh *et al.* (1988)
257.5, 87.5	1.0	5.5	14.8	6.3	7.2	8.2	23.4	Asudeh *et al.* (1988)

Crustal thickness in km, depths to various constant *P*-wave velocity surfaces (6.4, 6.8 and 7.2 km s^{-1}) in km, crustal *P*-wave surface velocity, the maximum lower crustal *P*-wave velocity, and the *Pn* velocity in $5^\circ \times 5^\circ$ cells where Lithoprobe seismic refraction data is available in Canada. The references are those from published results based on the Lithoprobe seismic refraction studies. The crustal thickness does not include sediment layers. The errors associated with the delineation of the Moho boundary are generally between 5 and 10 per cent of the total thickness. Errors associated with the delineation of *P*-wave velocity depths are generally within 0.1–0.2 km s^{-1} as given in the individual velocity models.

velocities across Canada in kilometres per second, which range from 7.6–8.3 km s^{-1} on a $5^\circ \times 5^\circ$ grid. It should be noted that some point values from the Lithoprobe data showed *Pn* as high as 8.6 km s^{-1}. Control points outside of Canada were established every 10° to act as bounding constraints for the spherical spline interpolation, and were assigned the value of the average depth of the particular *P*-wave surface. This regularization was necessary due to the sparsely distributed Lithoprobe data. As only depths to average velocities in the three crustal layers could be extracted from CRUST5.1, it was not possible to obtain depths to our chosen velocity surfaces, thus limiting these model attributes to cells within Canada where Lithoprobe results were available.

The crustal thickness of North America according to LITH5.0 is shown in Fig. 3(a). The region of thickest crust is located in the central Canadian Shield, where the maximum thickness reaches approximately 55 km beneath the mid-continent rift at Lake Superior. Fig. 3(b) shows the rms difference between the LITH5.0 and CRUST5.1 models. The most significant differences are seen in the northern Canadian Cordillera, the central Canadian Shield and the eastern Canadian Platform, all of which are well sampled by Lithoprobe seismic refraction surveys.

4 GEODYNAMIC IMPLICATIONS

Crustal modelling plays a fundamental role in the prediction of the isostatic surface topography, which is the large background topography resulting from isostatically compensated crustal heterogeneities. In contrast, the dynamic surface topography is maintained by all contributions to the topography due to density anomalies in the mantle (Forte *et al.* 1993). The observed surface topography of the planet consists of a linear superposition of this dynamic topography and the larger background topography due to the isostatic compensation of crustal heterogeneity. This background or isostatic topography must be thus removed from the observed surface topography in order to obtain the dynamic topography contribution. The latter may then be employed as a constraint on the density anomalies in the mantle. It is thus clear that accurate models of crustal heterogeneity are necessary to obtain reliable estimates of the surface dynamic topography.

The condition of isostasy, or surface mass compensation, requires that the total mass in any unit-area vertical column at the surface be constant down to a depth of compensation. This is the condition of hydrostatic equilibrium. It can be expressed in terms of the depth distribution of horizontal density anomalies $\Delta\rho(y)$ in the lithosphere as follows:

$$\int_0^h \Delta\rho(y)\, dy = 0 \tag{2}$$

where h is the thickness of the layer and y is the integration depth variable. In order to isolate the mantle or dynamic contribution to surface topography, it is necessary to remove the isostatically compensated crustal contribution.

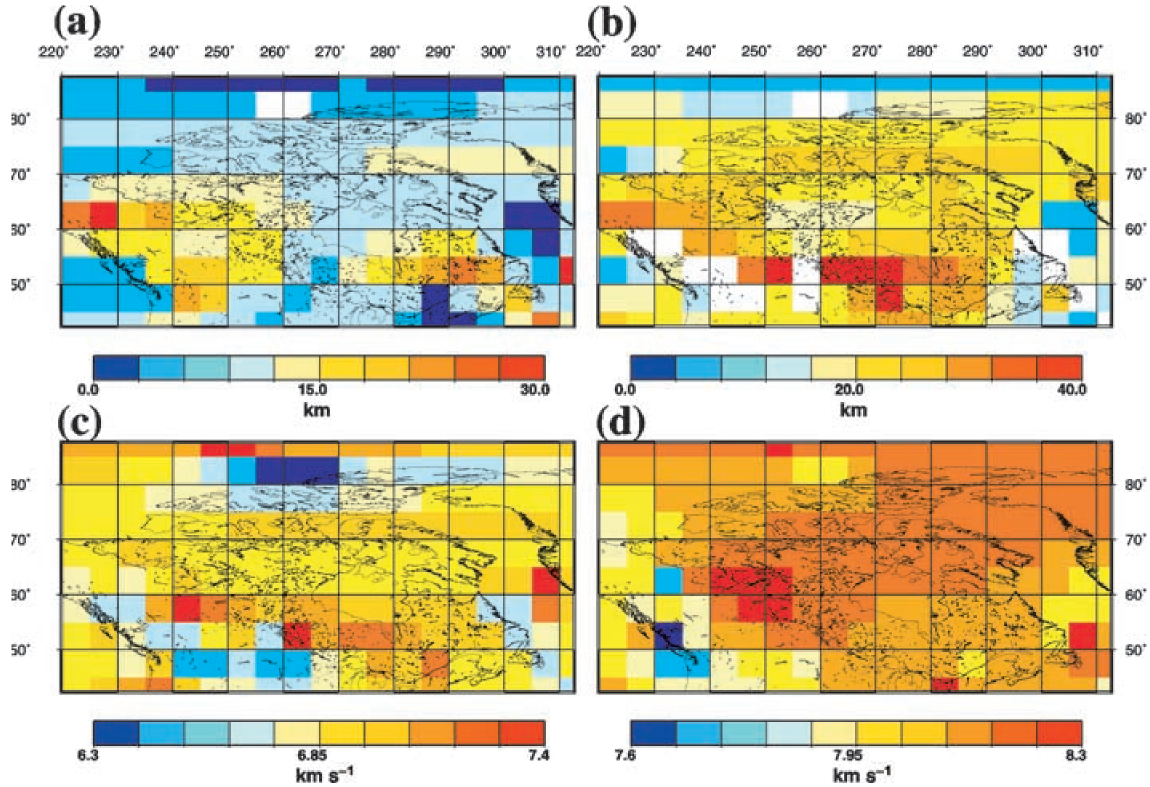

Figure 2. Depth to constant P-wave velocity surfaces, in km, from velocity–depth functions extracted from published crustal interpretations for (a) 6.4, (b) 6.8 km s^{-1}. (c) Maximum lower crustal velocity in km s^{-1}. (d) Mean Pn velocity in km s^{-1}. Pn velocities range from 7.6–8.3 km s^{-1} in $5^\circ \times 5^\circ$ cells in Canada, however some point values reach 8.6 km s^{-1}. Spherical spline interpolation was used to extrapolate values into regions lacking data. The values of the interpolated constant velocity surfaces and P-wave velocities for the 47 $5^\circ \times 5^\circ$ cells containing Lithoprobe constraints are listed in Table 1. Cells in white signify that the maximum crustal velocity was less than that of the contour value.

We apply to our model of crustal heterogeneity the isostasy principle as expressed in eq. (2). We use the LITH5.0 model of crustal thickness and crustal velocity structure in North America and convert P-wave velocities to densities via the velocity-to-density systematics presented in Christensen & Mooney (1995). These consist of linear regression lines derived from petrological and seismic constraints for various rock types. The estimate of isostatic topography, and hence the dynamic topography, is very sensitive to the P-wave velocity-to-density conversion scheme. In studying crustal densities, it is preferable to use a scheme for rocks excluding those of monomineralic or volcanic composition, since it is unlikely that they are abundant in crustal lithologies (Christensen & Mooney 1995). We thus considered the upper crustal section to typically contain granitic gneiss, becoming increasingly tonalitic with depth; a mid-crustal region characterized by abundant amphibolite; and a lower crustal region containing granulite facies assemblages grading to mafic garnet granulite.

The thicknesses of ice and water layers were taken from the CRUST5.1 model. Average values of density and V_P for the water layer were chosen to be 1.02 g cm^{-3} and 1.50 km s^{-1}, respectively, and 0.92 g cm^{-3} and 3.81 km s^{-1} for the ice layers, respectively (Bass 1995). Continental P-wave velocities of unconsolidated (soft) sediment and consolidated (hard) sediment were taken to be 2.0–3.0 and 4.0–5.3 km s^{-1}, respectively. Mooney *et al.* (1998) deemed it necessary to include two layers of sediments due to the range of seismic velocity properties in these layers and also due to the impact of low elastic velocities and densities of some sedimentary basins on all geophysical measurements. For further consultation of the data sources for water, ice and sediment layers, we refer the reader to Mooney *et al.* (1998). Through an averaging of the seismic properties of the crust, CRUST5.1 presents a piecewise constant velocity–depth model, whereas LITH5.0 presents a velocity model which is continuous with depth. Seismic velocities from these crustal models were converted to density using the velocity–density systematics of Christensen & Mooney (1995). Densities were integrated vertically through a cubic spline interpolation scheme. The calculation of these surface loads was an essential first step in the determination of geodynamic fields such as the dynamic surface.

In our application of the isostasy principle, expressed by eq. (2), we determined the depths to the Moho, the solid surface, and all intermediate crustal boundaries (which define the upper, middle and lower crust). On the basis of the boundary locations in the individual cells, we defined globally averaged values for the boundary locations and perturbations relative to these global averages. We used an upper-mantle density of 3.36 Mgm^{-3} as given by PREM (Dziewonski & Anderson 1981). Fig. 4(a) shows the isostatic surface topography for North America calculated on the basis of LITH5.0. The amplitude of its signal is comparable to that of the observed surface topography, however its shape is influenced by the crustal structure and thickness (see Fig. 3a). The dynamic topography (Fig. 4b) is calculated by subtracting the isostatic topography in Fig. 4(a) from the observed ETOPO5 (National Geophysical Data Center 1988) surface topography. This new determination of dynamic topography reinforces previous work sharing a significant large-scale depression of the central part of North America relative to its isostatic elevation (e.g. Forte *et al.* 1993; Forte & Perry 2000; Pari & Peltier 2000).

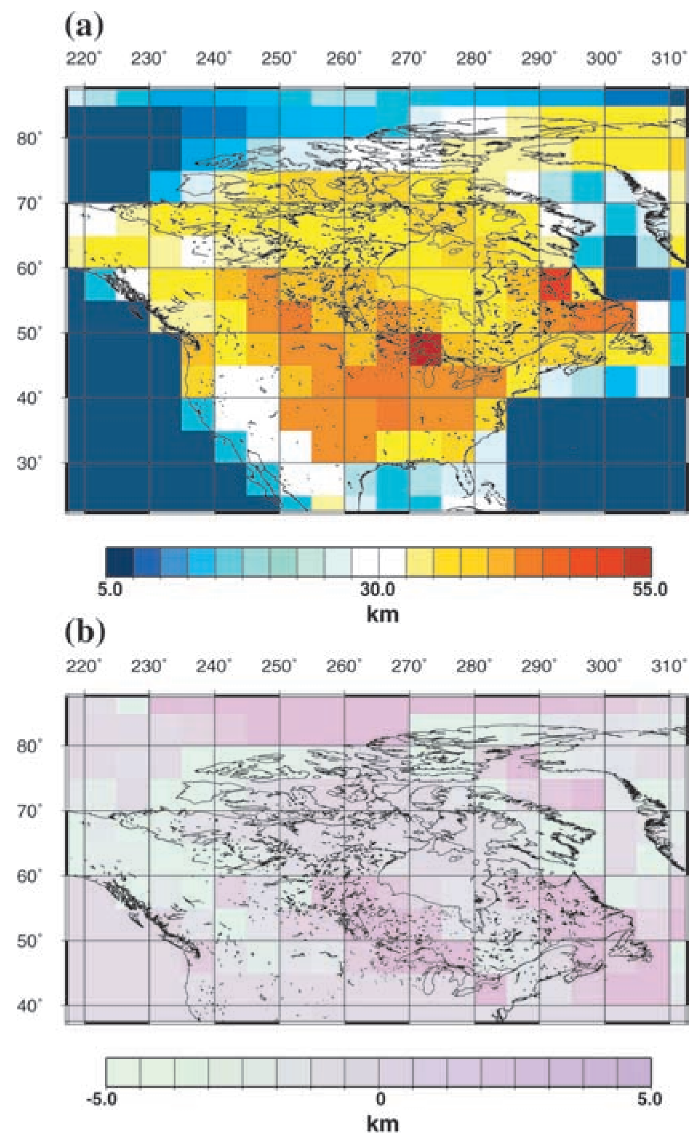

Figure 3. (a) Crustal Thickness of North America, in km, as predicted by the LITH5.0.Sediments are not included in the crustal model. (b) The rms difference, in km, between the LITH5.0and CRUST5.1 models. The average rms difference in regions constrained by Lithoprobe data is foundto be 5.5 km. In general, CRUST5.1 underestimates the thickness of the crust in parts of the centralCanadian Shield and over-estimates crustal thickness in regions of the northern Canadian Cordillera.

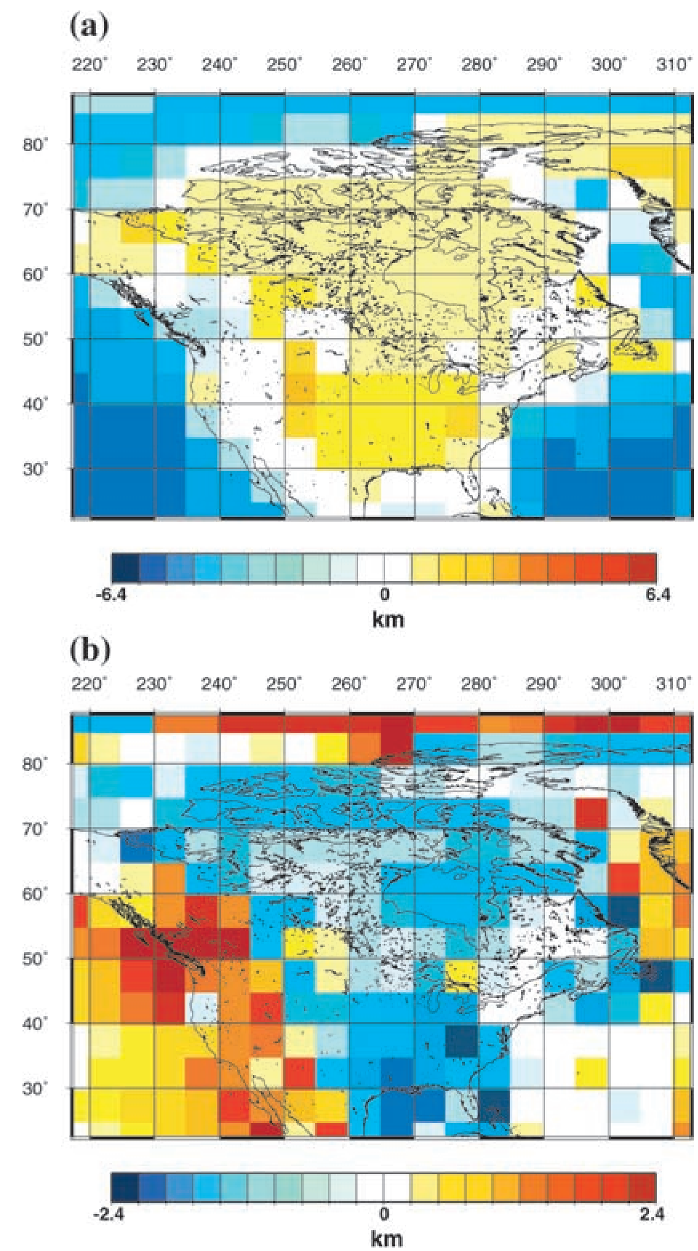

Figure 4. (a) Isostatic surface topography calculated on the basis of the LITH5.0 crustal model. (b)Dynamic or residual topography of North America obtained by subtracting the isostatic topography in(a) from the observed ETOPO5 surface topography.

The results of a more detailed analysis of the implications of North American dynamic topography are presented in Perry *et al.* (2002).

5 DISCUSSION

As expected, the *P*-wave velocities are generally higher within the cratonic nucleus of the continent, and the continental margins are characterized by lower seismic velocities. These reduced velocities are a result of the abundance of sedimentary rock sequences, subduction processes in the Western Cordillera and high heat flow due to tectonic activity in the region. Indeed, the *Pn* velocity may provide a proxy for the mantle heat flux and temperature. Recent results show that the high elevations in the northern Cordillera are supported by hot, buoyant upper mantle (Hyndman & Lewis 1999). The LITH5.0 model suggests a relatively thin crust (∼34 km) beneath the northern Canadian Cordillera, which is in agreement with this hypothesis. In contrast, CRUST5.1 suggests the presence of an Airy-type isostatic root beneath the northern Cordillera. The inconsistency between LITH5.0 and CRUST5.1 in the northern Cordillera contributes significantly to the 5.5 km rms difference between the models (see Fig. 3b).

Although crustal thickness trends in Canada exhibit a similar pattern for both LITH5.0 and CRUST5.1, important differences exist in certain areas where new data are available. The 5.5 km rms difference in crustal thickness is significant considering that the mean Moho depth (with respect to sea level) of continents predicted by CRUST5.1 is 38.0 km. The strongest differences in the models occur in the northern Canadian Cordillera and in regions of the central Canadian Shield (Fig. 3b). LITH5.0 shows a thicker crust in the southern Canadian Cordillera and mid-continent region, notably beneath the mid-continent rift at Lake Superior. The thin crust beneath the northern Canadian Cordillera is unexpected, given its high elevation. The LITH5.0 model is well sampled in western Canada, and suggests a northwardly thinning crust atop the cratonic root, with an annular girdle of thicker crust flanking its interior.

The Canadian Shield is an ancient geological terrane (>1.0 Ga) characterized by thin or non-existent Phanerozoic sedimentary cover. It forms the nucleus of the continent and roughly coincides with an inferred region of cold, chemically buoyant lithospheric mantle material (the so-called tectosphere) centred roughly on the western part of Hudson Bay (e.g. Forte & Perry 2000; Perry *et al.* 2002). With two notable exceptions, relatively thick crust (>42.5 km) in North America appears to occur mainly to the south and west of the cratonic nucleus, in areas where Phanerozoic sediments have accumulated in a platform setting (e.g. Mooney *et al.* 1998). This generalization applies even to areas where Archean basement rocks extend beneath the platform, such as in western Canada (approximately long. 250°E, lat. 50°N) (Villeneuve *et al.* 1993). The two exceptions are the extraordinarily thick crust in the mid-continental rift zone, centred on long. 272.5°E, lat. 47.5°N, and an area of thick crust in northern Quebec and Labrador centred approximately on long. 292.5°E, lat. 57.5°N.

In contrast to sedimentary platform regions to the south and west, the Canadian Shield is characterized by relatively thin crust (32.5–40.0 km) (Fig. 3a). Vestiges of Paleozoic rocks within kimberlite pipes that intrude the Archean Canadian Shield (e.g. Cookenboo *et al.* 1998) indicate that extensive areas of the Shield, perhaps all of it, were once covered by sedimentary rocks which have since been removed by uplift and erosion. Hence, it is tempting to speculate that the difference in crustal thickness between Shield and Platform regions in North America reflects the long-term dynamic behaviour of areas underlain by relatively buoyant tectospheric roots.

In the absence of tectonic influences such as the mid-continental rift, this interpretation predicts that a continuous annular girdle of thicker crust should encircle the Canadian Shield. Such an annular girdle is only partly evident given the existing data (Fig. 3a). We note, however, that crustal thickness to the north of Hudson Bay and hence the map patterns within the Canadian Arctic Islands are poorly constrained at present.

One major reason for the differences between LITH5.0 and CRUST5.1 is the improved seismic refraction data sets in Canada from Lithoprobe which were incorporated into the LITH5.0 model. This Lithoprobe data had not been incorporated into CRUST5.1, and the database from which CRUST5.1 was derived predates most of the Lithoprobe refraction surveys. In this regard, it is important to note that CRUST5.1 relies on globally averaged geological constraints, rather than direct seismic refraction constraints. By reducing the extent to which LITH5.0 is based on global geological averages, using instead the seismic refraction data, we can model the complexity of the crustal structure which defies a geological extrapolation scheme.

6 CONCLUSIONS

We have developed a new model for crustal thickness and velocity in Canada. It builds on the existing model, CRUST5.1, but incorporates recent Lithoprobe results. Unlike the CRUST5.1 model, we do not assume constant seismic velocities or densities for tectonic provinces where we lack data. Instead, the crustal data set has been interpolated using spherical splines such that smooth extrapolations with reasonable bounds may be obtained in regions lacking control. Spherical spline interpolation helps to avoid the problem of unconstrained, large-amplitude variations in Moho depth on a scale much less than $5^\circ \times 5^\circ$ in this region of North America. Differences between the two models are evident along the eastern Canadian Platform, and may result from the strong local variations in crustal thickness and Moho depth in this region. Large differences between the models are also seen in the northern Canadian Cordillera and central Canadian Shield. This new study of crustal thickness is justified in view of the 5.5 km rms difference between LITH5.0 and CRUST5.1 in areas of dense Lithoprobe coverage.

The cell size of our model, and that of CRUST5.1 (550 km by 550 km at the equator), does not allow accurate small-scale modelling of regional crustal features such as continental margins. Further seismic refraction studies in North America and the incorporation of other types of data (e.g. surface wave dispersion) will enlarge the geographical coverage of the crustal model and improve its resolution. The LITH5.0 model could also be improved by incorporating receiver function results into the current *P*-wave based model. The POLARIS project (Cassidy *et al.* 2000), which has been recently initiated in Canada will provide the means to incorporate teleseismic results into the existing crustal model, and it will provide new constraints on the structure of the Canadian crust on a finer grid.

ACKNOWLEDGMENTS

The LITH5.0 crustal model is available on the website http://www.gp.uwo.ca/deaton/lith. The authors thank R. M. Clowes, W. D. Mooney, and an anonymous reviewer for their constructive comments regarding the original manuscript. The authors are grateful to D. White for providing unpublished data and C. Woodgold for providing some initial references. The research was funded by the Canadian Natural Sciences and Engineering Research Council (NSERC) and Project Lithoprobe. HKCP is grateful for support provided by NSERC, the Society of Exploration Geophysicists (SEG) and the Canadian Society of Exploration Geophysicists (CSEG). DWSE and AMF are funded, in part, from individual NSERC Operating Grants. AMF acknowledges the support of the Earth System Evolution Program—Canadian Institute of Advanced Research. This is Lithoprobe publication no. 1270.

REFERENCES

Asudeh, I., Green, A.G. & Forsyth, D.A., 1988. Canadian expedition to study the Alpha Ridge Complex: results of the seismic refraction survey, *Geophys. J.,* **92,** 283–301.

Asudeh, I., Forsyth, D.A., Stephenson, R., Embry, E., Jackson, H.R. & White, D., 1989. Crustal structure of the Canadian polar margin: results of the 1985 seismic refraction survey, *Can. J. Earth. Sci.,* **26,** 853–866.

Bass, J.D., 1995. Elasticity of minerals, glasses, and melts, in *Mineral Physics and Crystallography: A Handbook of Physical Constants, AGU Ref. Shelf,* Vol. 2, pp. 45–63, ed. Ahrens, T.J., American Geophysical Union, Washington, DC.

Boland, A.V. & Ellis, R.M., 1991. A geophysical model for the Kapuskasing uplift from seismic and gravity studies, *Can. J. Earth. Sci.,* **28,** 342–354.

Cassidy, J.F. *et al.*, 2000. POLARIS: Portable Observatories for Lithospheric Analysis and Research Investigating Seismicity—A Canadian Proposal, *Seismological Society of America Annual Meeting,* San Diego, CA.

Chian, D. & Louden, K.E., 1992. The structure of Archean-Ketilidian crust along the continental shelf of southwestern Greenland from a seismic refraction profile, *Can. J. Earth. Sci.,* **29,** 301–313.

Chian, D. & Louden, K.E., 1994. The continent-ocean crustal transition across the southwest Greenland margin, *J. geophys. Res.,* **99,** 9117–9135.

Chian, D., Louden, K.E. & Reid, I., 1995. Crustal structure of the Labrador Sea conjugate margin and implications for the formation of nonvolcanic continental margins, *J. geophys. Res.,* **100,** 24 239–24 253.

Christensen, N.I. & Mooney, W.D., 1995. Seismic velocity structure and compostion of the continental crust: a global view, *J. geophys. Res.,* **100,** 9761–9788.

Clowes, R.M., Zelt, C.A., Amor, J.R. & Ellis, R.M., 1995. Lithospheric structure in the southern Canadian Cordillera from a network of seismic refraction lines, *Can. J. Earth. Sci.,* **32,** 1485–1513.

Clowes, R., Cook, F., Hajnal, Z., Hall, J., Lewry, J., Lucas, S. & Wardle, R., 1999. Canada's Lithoprobe Project (collaborative, multidisciplinary geoscience research leads to new understanding of continental evolution), *Episodes,* **22,** 3–20.

Cookenboo, H.O., Orchard, M.J. & Daoud, D.K., 1998. Remnants of Paleozoic cover on the Archean Canadian Shield; limestone xenoliths from kimberlite in the central Slave Craton, *Geology,* **26,** 391–394.

Creaser, B. & Spence, G., 2000. Crustal seismic velocity structure of the northern Cordillera, southern Yukon Territory—LITHOPROBE SNoRE Line 21, *Lithoprobe Report,* **72,** 110–113.

Delandro, W. & Moon, W., 1982. Seismic structure of the Superior-Churchill Precambrian boundary zone, *J. geophys. Res.,* **87,** 6884–6888.

Dziewonski, A.M. & Anderson, D.L., 1981. Preliminary reference Earth model, *Phys. Earth planet. Int.,* **25,** 297–356.

Ekström, G. & Dziewonski, A.M., 1998. The unique anisotropy of the Pacific upper mantle, *Nature,* **394,** 168–172.

Epili, D. & Mereu, R.F., 1989. Onshore refraction and wide-angle PmP observations from a fan profile over the Lake Superior Midcontinent Rift System, in *Earth's Lower Crust: Properties and Processes,* pp. 93–101, eds Mereu, R.M., Mueller, S. & Fountain, D., American Geophysical Union, Washington, DC.

Fernández Viejo, G. & Clowes, R.M., 2002. Lithospheric structure beneath the Archean Slave Province and Proterozoic Wopmay Orogen, north western Canada, from a LITHOPROBE refraction/wide-angle reflection survey, *Geophys. J. Int.,* (submitted to).

Forte, A.M. & Perry, H.K.C., 2000. Geodynamic evidence for a chemically depleted continental tectosphere, *Science,* **290,** 1940–1944.

Forte, A.M., Peltier, W.R., Dziewonski, A.M. & Woodward, R.L., 1993. Dynamic surface topography: a new interpretation based upon mantle flow models derived from seismic tomography, *Geophys. Res. Lett.,* **20,** 225–228.

Forte, A.M., Dziewonski, A.M. & O'Connell, R.J., 1995. Continent-ocean chemical heterogeneity in the mantle based on seismic tomography, *Science,* **268,** 386–388.

Funck, T. & Louden, K.E., 1999. Wide-angle seismic transect across the Torngat Orogen, northern Labrador: evidence for a Proterozoic crustal root, *J. geophys. Res.,* **104,** 7463–7480.

Funck, T., Louden, K.E. & Reid, I.D., 2000a. Wide-angle seismic imaging of a Mesoproterozoic anorthosite complex: The Nain Plutonic Suite in Labrador, Canada, *J. geophys. Res.,* **105,** 25 693–25 707.

Funck, T., Louden, K.E., Wardle, R.J., Hall, J., Hobro, J.W., Salisbury, M.H. & Muzzatti, A., 2000b. Three-dimensional structure of the Torngat Orogen (NE Canada) from active seismic tomography, *J. geophys. Res.,* **105,** 23 403–23 420.

Grand, S.P., van der Hilst, R.D. & Widiyantoro, S., 1997. Global seismic tomography: a snapshot of convection in the Earth, *GSA Today,* **7,** 1–7.

Grandjean, G., Wu, H., White, D., Mareschal, M. & Hubert, C., 1995. Crustal velocity models for the Archean Abitibi greenstone belt from seismic refraction data, *Can. J. Earth. Sci.,* **32,** 149–166.

Hahn, A., Ahrendt, H., Meyer, J. & Hufen, J.-H., 1984. A model of magnetic sources within the Earth's crust compatible with the field measured by the satellite Magsat, *Geol. Jahrb., Reihe A,* **75,** 125–156.

Hall, J., Marillier, F. & Dehler, S., 1998. Geophysical studies of the structure of the Appalachian orogen in the Atlantic borderlands of Canada, *Can. J. Earth. Sci.,* **35,** 1205–1221.

Hammer, P.T.C. & Clowes, R.M., 1999. Crustal structure across the Cordilleran Orogen of northwest British Columbia: preliminary results of LITHOPROBE SNorCLE Refraction Experiment Line 22, *Lithoprobe Report,* **69,** 275–280.

Holbrook, W.S., Mooney, W.D. & Christensen, N.I., 1992. The seismic velocity structure of the lower continental crust, in *The Lower Continental Crust,* pp. 1–43, eds Fountain, D.M., Arculus, R., & Kay, R., Elsevier, New York.

Hughes, S. & Luetgert, J.H., 1992. Crustal structure of the southeastern Grenville Province, northern New York State and eastern Ontario, *J. geophys. Res.,* **97,** 17 455–17 479.

Hughes, S., Hall, J. & Luetgert, J.H., 1994. The seismic velocity structure of the Newfoundland Appalachian orogen, *J. geophys. Res.,* **99,** 13 633–13 653.

Hyndman, R.D. & Lewis, T.J., 1999. Geophysical consequences of the Cordillera-Craton thermal transition in southwestern Canada, *Tectonophysics,* **306,** 397–422.

Kaban, M.K. & Mooney, W.D., 2001. Density structure of the lithosphere in the Southwestern United States and its tectonic significance, *J. geophys. Res.,* **106,** 721–739.

Louden, K.E. & Fan, J., 1998. Crustal structures of Grenville, Makkovik, and southern Nain provinces along the Lithoprobe ESCOOT Transect: regional seismic refraction and gravity models and their tectonic implications, *Can. J. Earth. Sci.,* **35,** 583–601.

Mair, J.A. & Lyons, J.A., 1981. Crustal structure and velocity anisotropy beneath the Beaufort Sea, *Can. J. Earth. Sci.,* **18,** 724–741.

Marillier, F. & Reid, I., 1990. Crustal underplating beneath the Carboniferous Magdalen Basin (eastern Canada): evidence from seismic reflection and refraction, in *The Potential for Deep Seismic Profiling for Hydrocarbon Exploration,* pp. 209–218, eds Pinet, B. & Bois, C., Editions Technip, Paris.

Marillier, F. *et al.*, 1994. Lithoprobe East onshore-offshore seismic refraction survey—constraints on interpretation of reflection data in the Newfoundland Appalachians, *Tectonophysics,* **232,** 43–58.

McMechan, G.A. & Spence, G.D., 1983. P-wave structure of the Earth's crust beneath Vancouver Island, *Can. J. Earth. Sci.,* **20,** 742–752.

Mégnin, C. & Romanowicz, B., 2000. The three-dimensional shear velocity structure of the mantle from inversion of body, surface and higher-mode wave forms, *Geophys. J. Int.,* **143,** 709–728.

Mereu, R. *et al.*, 1986. The 1982 COCRUST seismic experiment across the Ottawa-Bonnechere graben and Grenville Front in Ontario and Quebec, *Geophys. J. R. astr. Soc.,* **84,** 491–514.

Mooney, W.D., 1989. Seismic methods for determining earthquake source parameters and lithospheric structure, in *Geophysical Framework of the Continental United States,* 11–34, eds Pakiser, L.C. & Mooney, W.D., *Mem. Geol. Soc. Am.,* Boulder, CO.

Mooney, W.D. & Braile, L.W., 1989. The seismic structure of the continental crust and upper mantle of North America, in *The Geology of North America, Overview,* Vol. A, pp. 39–52, eds Bally, A.W. & Palmer, A.R., *Geol. Assoc. Am.,* Boulder, CO.

Mooney, W.D., Laske, G. & Masters, T.G., 1998. CRUST5.1: a global crustal model at $5^\circ \times 5^\circ$ *J. geophys. Res.,* **103,** 727–747.

Nataf, H.-C. & Ricard, Y., 1996. 3SMAC: AN a priori tomographic model of the upper mantle based on geophysical modeling, *Phys. Earth planet. Int.,* **95,** 101–122.

National Geophysical Data Center, 1988. ETOPO-5, bathymetry/topography data, *Data Announc.,* 88-MGG-02, Natl. Oceanic and Atmos. Admin., U.S. Dep. of Commer., Washington, DC., 1988.

Németh, B. & Hajnal, Z., 1998. Moho signature from wide-angle reflections: preliminary results of the 1993 Trans-Hudson Orogen refraction experiment, *Tectonophysics,* **288,** 93–104.

Pari, G. & Peltier, W.R., 2000. Subcontinental mantle dynamics: a further analysis based on the joint constraints of dynamic surface topography and free-air gravity, *J. geophys. Res.,* **105,** 5635–5662.

Parker, R.L., 1994. *Geophysical Inverse Theory,* Princeton University Press, NJ.

Perry, H.K.C., Forte, A.M. & Eaton, D.W.S., 2002. Constraints on mantle dynamics below North America from tomography-based flow models: Implications of dynamic topography and free-air gravity anomalies, *Geophys. J. Int.,* (submitted to).

Reid, I.D., 1994. Crustal structure of a nonvolcanic rifted margin east of Newfoundland, *J. geophys. Res.,* **99,** 15 161–15 180.

Reid, I., 1996. Crustal structure across the Nain-Makkovik boundary on the continental shelf off Labrador from seismic refraction data, *Can. J. Earth. Sci.,* **33,** 460–471.

Shapiro, S.S., Hager, B.H. & Jordan, T.H., 1999. Stability and dynamics of the continental tectosphere, *Lithos,* **48,** 115–133.

Soller, D.R., Ray, R.D. & Brown, R.D., 1982. A new global crustal thickness model, *Tectonics,* **1,** 125–149.

Spence, G.D. & Asudeh, I., 1993. Seismic velocity structure of the Queen Charlotte Basin beneath Hecate Strait, *Can. J. Earth. Sci.,* **30,** 787–805.

Tanimoto, T., 1995. Crustal structure of the Earth, *Global Earth Physics: A Handbook of Physical Constants, AGU Ref. Shelf,* Vol. 1, pp. 214–224, ed. Ahrens, T.J., AGU, Washington, DC.

Villeneuve, M.E., Ross, G.M., Theriault, R.J., Miles, W., Parrish, R.R. & Broome, J., 1993. Tectonic subdivision and U-Pb geochronology of the crystalline basement of the Alberta Basin, Western Canada, *Geological Survey of Canada Bulletin,* p. 93, Geological Survey of Canada, Ottawa.

Welford, J.K., Clowes, R.M., Ellis, R.M., Spence, G.D., Asudeh, I. & Hajnal, Z., 2001. Lithospheric structure across the craton-Cordilleran transition of northeastern British Columbia, *Can. J. Earth. Sci.,* **38,** 1169–1189.

Winardhi, S. & Mereu, R.F., 1997. Crustal velocity structure of the Superior and Grenville provinces of the southeastern Canadian Shield, *Can. J. Earth. Sci.,* **34,** 1167–1184.

Zelt, B.C. *et al.*, 1992. Crust and upper mantle velocity structure of the Intermontane belt, southern Canadian Cordillera, *Can. J. Earth. Sci.,* **29,** 1530–1548.

Zelt, C.A. & Ellis, R.M., 1989. Seismic structure of the crust and upper mantle in the Peace River Arch Region, Canada, *J. geophys. Res.,* **94,** 5729–5744.

Zelt, C.A. & White, D.J., 1995. Crustal structure and tectonics of the southeastern Canadian Cordillera, *J. geophys. Res.,* **100,** 24 255–24 273.

Zelt, C.A., Forsyth, D.A., Milkereit, B., White, D.J., Asudeh, I. & Easton, R.M., 1994. Seismic structure of the Central Metasedimentary Belt, southern Grenville Province, *Can. J. Earth. Sci.,* **31,** 243–254.